Progress In Electromagnetics Research, PIER 103, 393–401, 2010

A COMPACT POLARIZATION BEAM SPLITTER BASED ON A MULTIMODE PHOTONIC CRYSTAL WAVEGUIDE WITH AN INTERNAL PHOTONIC CRYSTAL SECTION

Y. C. Shi

Centre for Optical and Electromagnetic Research
State Key Laboratory for Modern Optical Instrumentation
Joint Research Laboratory of Optics of Zhejiang Normal University and Zhejiang University
Zhejiang University
Zijingang Campus, East Building No. 5, Hangzhou 310058, China

Abstract—We present the design and simulation of an ultra-compact polarization beam splitter (PBS) by combining a photonic crystal (PhC) multimode waveguide and an internal PhC section. The PhC multimode waveguide is designed to collect the powers reflected by or transmitted through the internal PhC structure which serves as a polarization sensitive scatterer. Plane wave expansion (PWE) method is used to calculate the band structure and the finite-difference time-domain (FDTD) method is employed to obtain the spectrum response. The simulation results show that the present design can give an ultra-compact PBS with high extinction ratio over a broad bandwidth.

1. INTRODUCTION

A polarization beam splitter (PBS), which can separate the two orthogonal polarizations of light, is one of the most important components in modern optical communication systems. Various PBS's have been reported. The fabrication of the PBS based on an asymmetrical Y-Junction structure [1] or Mach-Zehnder interferometer (MZI) [2] requires complex processes such as photobleaching and poling.The PBS based on directional couplers [3] and conventional multimode interference (MMI) couplers [4] usually have a large size since the total length should be integer multiples of the coupling lengths for both polarizations. In recent years, photonic crystals (PhCs) [5–8] have been extensively investigated aiming at

Corresponding author: Y. C. Shi (yaocheng@zju.edu.cn).

the realization of high efficient ultra-compact photonic components. Recently, several types of PBS based on PhCs have been reported [9–12]. However, most of them only deal with the splitting structure. If these PBSs are used in an optical system, extra input/output waveguides have to be added. This will enlarge the size of the PBS, reduce the efficiency, and make the PBS less attractive.

Kim et al. reported that the self-imaging phenomenon is still available in a multimode PhC waveguide [13] as in a conventional multimode waveguide. A device based on the MMI effect in PhC can be much smaller than a conventional MMI device due to the large dispersion of a PhC structure. PhC-based MMI structures have been successfully used in, e.g., power splitters [14], optical switches [15], and demultiplexers [16]. To realize a multimode PhC waveguide based PBS, both transverse-electric (TE) and transverse-magnetic (TM) polarized light must propagate with low loss in the PhC structure. Thus, a PhC structure with an absolute photonic bandgap (PBG) is required. Many works have been reported on the realization of a complete PBG PhC [17–19]. In this work, we use a uniaxial crystal as the dielectric host to construct an anisotropic PhC which has a large absolute PBG [19]. We introduce an internal PhC section inside the PhC multimode region. The internal PhC section is designed to be polarization sensitive so that one polarization is reflected and the other one is transmitted through the internal PhC section. By using such a polarization sensitive PhC scatterer, there is no need to meet the common multiple for the two polarizations and the total device size could be reduced dramatically. Furthermore, the position of the PhC scatterer is no need to be integral multiples of the period.

2. DESIGN AND ANALYSIS

Figure 1 shows the schematic configuration of the proposed PBS based on a PhC multimode waveguide with an internal PhC section. It consists of input/output PhC wavguides, a multimode PhC waveguide and an internal PhC section.

It has been proved that self-imaging phenomenon occurs in a PhC multimode waveguide [12]. The field distribution $\psi(x, z)$ in the PhC multimode waveguide can be written as a superposition of all the guided-modes of the multimode waveguide, i.e.,

$$\psi(x, z) = \sum_{\nu} c_\nu \phi_\nu(x) \exp[j(\beta_0 - \beta_v)z], \tag{1}$$

where c_ν and $\phi_\nu(x)$ are the excitation coefficient and modal field of the v-th order mode, respectively, β_0 and β_v are the propagation

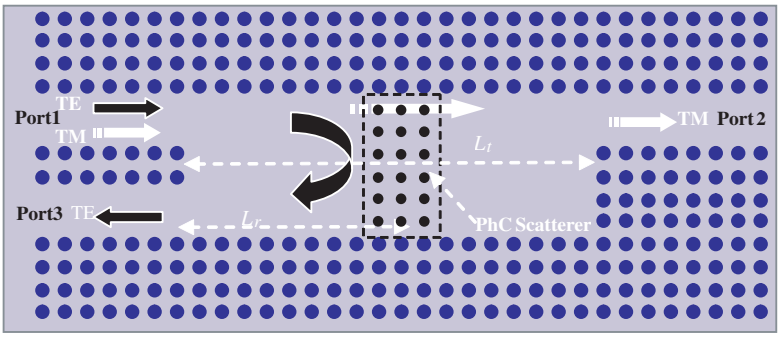

Figure 1. The schematic configuration of the proposed PBS.

constants of the fundamental mode and the v-th order mode. An input field profile can be reproduced in the form of direct images and mirrored images at periodic intervals along the path of propagation. The direct images position L_d and the mirrored images position L_m are determined by:

$$(\beta_0 - \beta_v)L_d = 2p_n\pi, \quad \text{with } p_n = 1, 2, 3 \ldots \quad (2)$$

$$\begin{array}{ll} (\beta_0 - \beta_v)L_m = 2q_n\pi & \text{for even modes} \\ (\beta_0 - \beta_v)L_m = (2q_n - 1)\pi & \text{for odd modes} \end{array}, \quad \text{with } q_n = 1, 2, 3 \ldots \quad (3)$$

In this paper, the PhC multimode waveguide works similar to a regular MMI splitter while the internal PhC section works as a polarization sensitive scatterer: high reflection for TE mode but high transmission for the TM mode. By assuming the transmission coefficient t and reflection coefficient r of the internal PhC section to be the same for all the guided-modes, the forward propagating field $\psi_t(x, L_t)$ at Port 2 and the backward propagating field $\psi_r(x, 0)$ at Port 3 is given by

$$\begin{array}{l} \psi_t(x, L_t) = t \cdot \sum_\nu c_\nu \phi_\nu(x) \exp[j(\beta_0 - \beta_v)L_t] \\ \psi_r(x, 0) = r \cdot \sum_\nu c_\nu \phi_\nu(x) \exp[j(\beta_0 - \beta_v) \cdot 2 \cdot L_r] \end{array}, \quad (4)$$

where L_t is the total length of the MMI section and L_r is the distance between the start of the PhC MMI and the beginning of the internal PhC section, (see Fig. 1). By choosing $L_t = L_d^{TM}$ and $L_r = L_m^{TE}/2$ (L_m^{TE} and L_d^{TM} are the first mirrored image and first direct image position for TE and TM polarization, respectively), we

obtain

$$\begin{aligned} \psi_t(-x, L_t) &= t \cdot \psi(-x, 0) \\ \psi_r(x, 0) &= r \cdot \psi(-x, 0) \end{aligned}, \tag{5}$$

where $\psi(-x, 0)$, $\psi_t(-x, L_t)$ and $\psi_r(x, 0)$ are the input field, the forward propagating field and the backward propagating field, respectively; t and r are the transmission coefficient and the reflection coefficient of the internal PhC section. From Eq. (5), one easily find that there are single-fold self-images at the forward and backward directions for different polarizations if the internal PhC section is designed to exhibit a large reflection coefficient for TE and a high transmission coefficient for TM polarization (i.e., $t_{TE} \approx 0$, $r_{TE} \approx 1$, $t_{TM} \approx 1$, $r_{TM} \approx 0$).

3. SIMULATION AND DISCUSSION

To realize a PBS, both TE and TM polarizations should propagate with low loss in the PhC waveguides. Therefore, a PhC structure with a complete bandgap is required. It has been reported in [19] that a 2D anisotropic PhC using a uniaxial crystal as the dielectric material can have a large absolute bandgap. In this work, we use a 2D anisotropic PhC with the same geometry parameters as that in [19]. The positive uniaxial crystal Te (tellurium) with principal indices of $n_e = 6.2$ and $n_o = 4.8$ is considered. The PhC structures are formed by a square lattice of Te rods in air. A complete PBG is obtained in a frequency range of 0.219–0.254 ($2\pi c/a$) when the radius of the dielectric rods is chosen to be $r = 0.357a$ (a is the lattice constant). The multimode

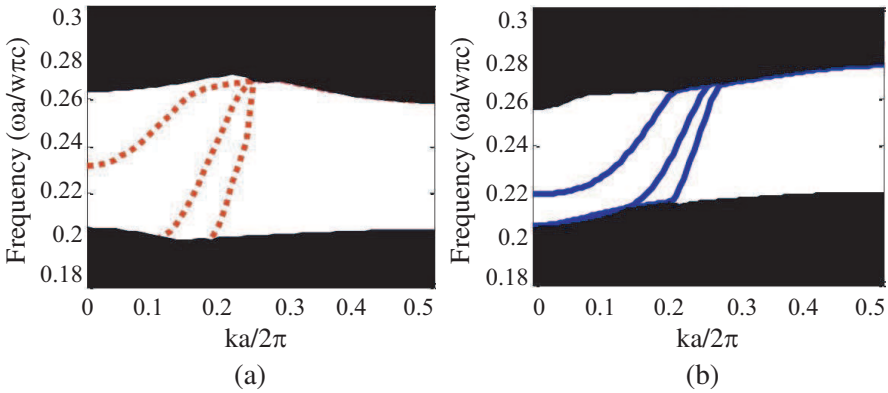

Figure 2. The projected band diagram for the W6 PhC waveguide for (a) TE polarization; (b) TM polarization.

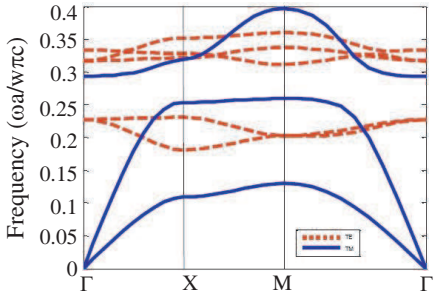

Figure 3. The band diagrams of the internal PhC section. The dotted and solid lines represent the polarization bands of TE and TM polarizations, respectively.

section surrounded by PhC was formed by removing six consecutive rows from a square lattice. Plane wave expansion (PWE) method is used to calculate the band structure. The projected band diagram of the multimode region in PhC for TE and TM polarizations are shown in Fig. 2. From the figure, one could find that there are totally three guided modes (the dotted and solid curves are the dispersion relations for guided modes of TE and TM polarizations, respectively).

From (5), we can find that the internal PhC section should exhibit a large reflection coefficient for TE and a high transmission coefficient for TM polarization (i.e., $t_{TE} \approx 0$, $r_{TE} \approx 1$, $t_{TM} \approx 1$, $r_{TM} \approx 0$). From our analysis, we find that a square lattice with 3×6 rods with air $r/a = 0.3$ can be utilized as such a positive sensitive scatterer. Fig. 3 shows the band diagram for the internal PhC section. One could find that such a PhC structure exhibit PBG for TE polarization within the frequency range from 0.23 $(2\pi c/a)$ to 0.26 $(2\pi c/a)$ while no bandgap for TM polarization.

By using a 2-D finite-difference time-domain (FDTD) method with perfectly matched layer (PML) boundary treatment [20], we carry out numerical simulations for the light propagation in the proposed PBS. The PhC multimode length could only be chosen in terms of lattice periodicity. Thus, the length of the multimode section is determined to be $L_t = L_d^{TM} = 33a$ where the first direct image is formed for TM polarization at working frequency $f = 0.236(2\pi c/a)$. For the TE polarization, the first mirrored image would be formed at $L_m^{TE} = 30.4a$. From the analysis in Section 2, we find that the position of the internal PhC section could be easily determined by $L_r = L_m^{TE}/2$. The length of the internal PhC section is chosen to be three periods to ensure large enough reflection for TE polarization while keeping high transmission

for TM polarization at the same time. Thus, the total device size is only $50a$ including the input/output waveguides, while a common multiple for TE and TM polarization makes the device quite large with a conventional design. Furthermore, it is rather difficult to find an exact multimode section length at which a mirrored image and a direct image are formed for TE and TM polarizations in a conventional design.

Figure 4 shows the FDTD simulated steady-state field distribution in the proposed PBS for both TE and TM polarizations at working frequency $f = 0.236(2\pi c/a)$. For TM polarization, the light transmits through the internal PhC section with high transmission efficiency and finally a direct image is formed at Port 2. For TE polarization, the input light from Port1 are reflected back by the internal PhC

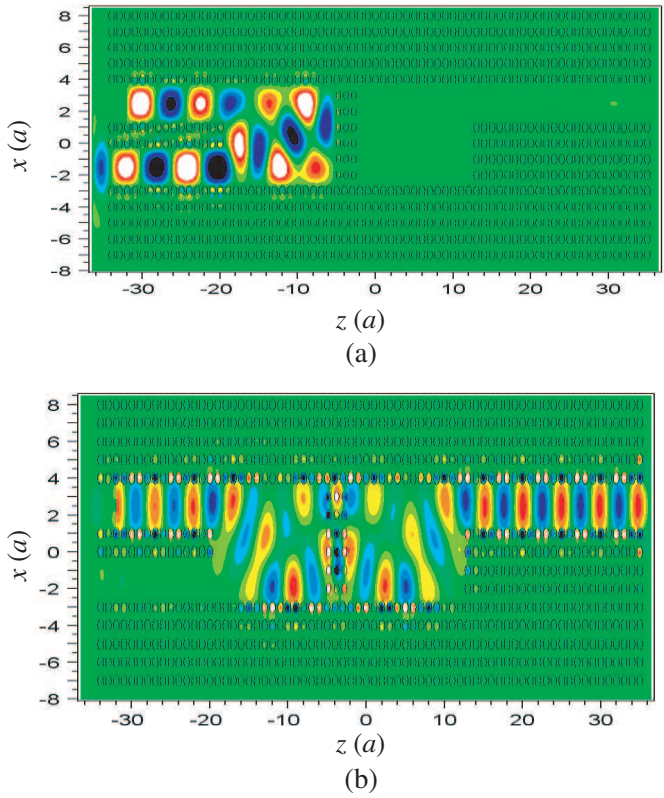

Figure 4. FDTD simulation for the field distribution at frequency $f = 0.236(2\pi c/a)$ in the present PBS (a) TE Polarization; (b) TM Polarization.

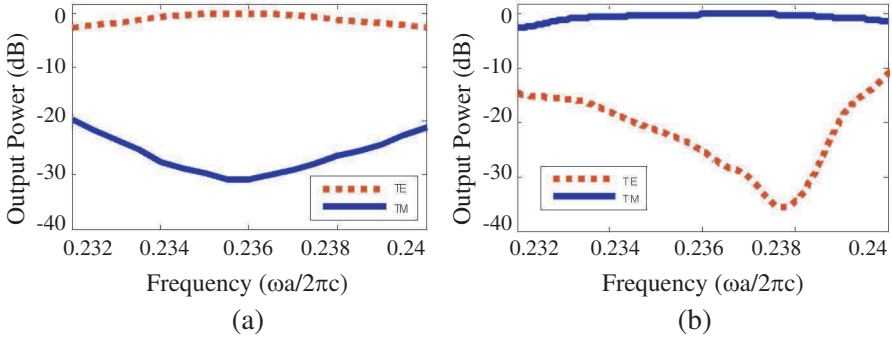

Figure 5. The output powers from the two output ports varies with the wavelength for both polarizations (a) Port 3; (b) Port 2.

section with high reflection efficiency and finally collected by Port 3. Therefore, one could find that the polarization splitting function was performed successfully.

To further characterize the PBS, the transmission spectra for both TE and TM polarizations are calculated with FDTD. The output power from Port 2 and Port 3 are normalized to the input power. The spectrum response of the PBS is given in Fig. 5. From the figure, we could find an insertion loss of 0.05 and 0.2 dB as well as an extinction ratio of 30.8 and 25.5 dB for TE and TM polarization at working frequency $f = 0.236(2\pi c/a)$, respectively. The spectrum shows the designed PBS has good performance over the frequency range from $0.232(2\pi c/a)$ to $0.24(2\pi c/a)$. If the central working wavelength is chosen to be 1.55 μm ($a = 0.236 \times 1.55 = 0.3658$ μm), a bandwidth larger than 50 nm can be achieved.

4. CONCLUSION

An ultra-compact PBS has been designed by combining PhC multimode waveguides with an internal PhC section. The introduction of the internal PhC section makes the design much more flexible since the length of the multimode waveguide region is no longer needed to be integral multiples of the coupling lengths for any polarization. Good performances such as low insertion loss and high extinction ratio are verified by FDTD simulation.

ACKNOWLEDGMENT

This work was partially supported by the National Nature Science Foundation of China (60907018) and by the China Postdoctoral Science Foundation (20080440198). The author would also like to acknowledge Prof. Sailing He for helpful discussions.

REFERENCES

1. Hu, M. H., Z. Huang, R. Scarmozzino, M. Levy, and R. M. Osgood, Jr., "Tunable Mach-Zehnder polarization splitter using height-tapered Y-branches," *IEEE Photon. Technol. Lett.*, Vol. 9, No. 6, 773–775, 1997.
2. Soldano, L. B., A. H. de Vreede, M. K. Smit, B. H. Verbeek, E. G. Metaal, and F. H. Groen, "Mach-Zehnder interferometer polarization splitter in InGaAsP-InP," *IEEE Photon. Technol. Lett.*, Vol. 6, No. 3, 402–405, 1994.
3. Kiyat, I., A. Aydinli, and N. Dagli, "A compact silicon-on-insulator polarization splitter," *IEEE Photon. Technol. Lett.*, Vol. 17, No. 1, 100–102, 2005.
4. Hong, J. M., H. H. Ryu, S. R. Park, J. W. Jeong, S. G. Lee, E.-H. Lee, S.-G. Park, D. Woo, S. Kim, and B.-H. O, "Design and fabrication of a significantly shortened multimode interference coupler for polarization splitter application," *IEEE Photon. Technol. Lett.*, Vol. 15, No. 1, 72–75, Jan. 2003.
5. Minin, I. V., O. V. Minin, Y. R. Triandaphilov, and V. V. Kotlyar, "Subwavelength diffractive photonic crystal lens," *Progress In Electromagnetics Research B*, Vol. 7, 257–264, 2008.
6. Srivastava, R., S. Pati, and S. P. Ojha, "Enhancement of omnidirectional reflection in photonic crystal heterostructures," *Progress In Electromagnetics Research B*, Vol. 1, 197–208, 2008.
7. Maleki Javan, A. R. and N. Granpayeh, "Fast Terahertz wave switch/modulator based on photonic crystal structures," *Journal of Electromagnetic Waves and Applications*, Vol. 23, No. 2–3, 203–212, 2009.
8. Srivastava, R., S. Srivastava, and S. P. Ojha, "Negative refraction by photonic crystal," *Progress In Electromagnetics Research B*, Vol. 2, 15–26, 2008.
9. Awasthi, S. K. and S. P. Ojha, "Wide-angle broadband plate polarizer with 1D photonic crystal," *Progress In Electromagnetics Research*, PIER 88, 321–335, 2008.
10. Ao, X. and S. He, "Polarization beam splitters based on a two-

dimensional photonic crystal of negative refraction," *Opt. Lett.*, Vol. 30, No. 16, 2152–2154, 2005.

11. Kim, S., G. P. Nordin, J. Cai, and J. Jiang, "Ultracompact high-efficiency polarizing beam splitter with a hybrid photonic crystal and conventional waveguide structure," *Opt. Lett.*, Vol. 28, No. 23, 2384–2386, 2003.
12. Li, Y., P. Gu, M. Li, H. Yan, and X. Liu, "Research on the wide-angle and broadband 2D photonic crystal polarization splitter," *Journal of Electromagnetic Waves and Applications*, Vol. 20, No. 2, 265–273, 2008.
13. Kim, H.-J., I. Park, B.-H. O, S.-G.Park, E.-H. Lee, and S.-G. Lee, "Self-imaging phenomena in multi-mode photonic crystal line-defect waveguides: Application to wavelength de-multiplexing," *Opt. Express*, Vol. 12, No. 23, 5625–5633, 2003.
14. Liu, T., A. R. Zakharian, M. Fallahi, J. V. Moloney, and M. Mansuripur, "Multi-mode interference-based photonic crystal waveguide power splitter," *J. Lightwave Technol.*, Vol. 22, No. 12, 2842–2846, 2004.
15. Li, Z., Y. Zhang, and B. Li, "Terahertz photonic crystal switch in silicon based on self-imaging principle," *Opt. Express*, Vol. 14, No. 9, 3887–3892, 2006.
16. Banaei, H. A. and A. Rostami, "A novel proposal for passive all-optical demultiplexer for DWDM systems using 2-D photonic crystals," *Journal of Electromagnetic Waves and Applications*, Vol. 22, No. 4, 471–482, 2008.
17. Qiu, M. and S. He, "Optimal design of a two-dimensional photonic crystal of square lattice with a large complete two-dimensional bandgap," *J. Opt. Soc. Am. B*, Vol. 17, No. 6, 1027–1030, 2000.
18. Hsu, S., M. Chen, and H. Chang, "Investigation of band structures for 2D non-diagonal anisotropic photonic crystals using a finite element method based eigenvalue algorithm," *Opt. Express*, Vol. 15, No. 12, 5416–5430, 2007.
19. Li, Z., B. Gu, and G. Yang, "Large absolute band gap in two-dimensional anisotropic photonic crystals," *Phys. Rev. Lett.*, Vol. 81, 2574–2577, 1998.
20. Taflove, A., *Computational Electromagnetics: The Finite-difference Time-domain Method*, Artech House, Norwood, MA, 1995.